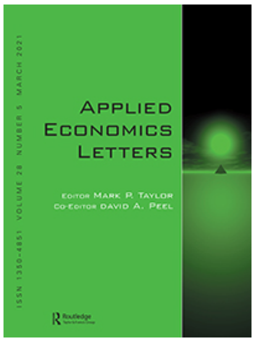

Applied Economics Letters

ISSN: (Print) (Online) Journal homepage: https://www.tandfonline.com/loi/rael20

Robust coherence analysis for long-memory processes

Yaeji Lim & Hee-Seok Oh

To cite this article: Yaeji Lim & Hee-Seok Oh (2021) Robust coherence analysis for long-memory processes, Applied Economics Letters, 28:5, 335-342, DOI: 10.1080/13504851.2020.1730749

To link to this article: https://doi.org/10.1080/13504851.2020.1730749

Published online: 23 Feb 2020.

APPLIED ECONOMICS LETTERS
2021, VOL. 28, NO. 5, 335–342
https://doi.org/10.1080/13504851.2020.1730749

Routledge
Taylor & Francis Group

ARTICLE

Check for updates

Robust coherence analysis for long-memory processes

Yaeji Lim[a] and Hee-Seok Oh[b]

[a]Department of Applied Statistics, Chung-Ang University, Seoul, Korea; [b]Department of Statistics, Seoul National University, Seoul, Korea

ABSTRACT
This paper investigates the linear relationships between two time-series in the frequency domain, termed coherence analysis. It is widely used in various fields, including signal processing, engineering, and meteorology. However, conventional coherence analysis tends to be sensitive to outliers. Laplace cross-periodogram and a corresponding robust coherence analysis based on the least-absolute deviation (LAD) regression have recently been developed to improve this shortcoming. In this paper, to extend the scope of Laplace cross-periodogram, we study a robust cross periodogram for long-memory processes and derive its asymptotic distribution. Through numerical studies, we demonstrate the usefulness of the proposed robust coherence analysis for long-memory processes.

KEYWORDS
Cross-spectrum; Laplace cross-periodogram; long-memory process; robust coherence analysis

JEL CLASSIFICATION
C13; C22

I. Introduction

The primary purpose of the cross-spectral analysis is to quantify how the variabilities of two time series are interrelated in the frequency domain. In general, the cross-spectral analysis is performed using a phase spectrum and coherence (coherency spectrum). In this paper, we focus on coherence, which is a measure of the degree of similarity between two signals in the frequency domain rather than the time domain, so that it may be influenced by the information of power and phase relations from the two signals. Coherence is widely used for analysing multiple time series that are observed from various fields, including meteorology, communications, and biology (Carter 1987; Grinsted, Moore, and Jevrejeva 2004; Sun, Miller, and D'Esposito 2004; Govindan et al. 2005; Maharaj and D'Urso 2010).

It is well known that the ordinary coherence analysis based on a cross-periodogram is efficient for cases that satisfy the Gaussian assumption; however, it suffers from considerable degradation in performance when the series follows a heavy-tailed or asymmetric distribution. To overcome such a problem, Li (2010) proposed Laplace cross-periodogram and its related concepts, which are more robust to outliers that might follow a heavy-tailed process.

Long-memory is a common situation that we encounter in analysing time series data. If the rate of decay of the statistical dependence of two points in the time series is slower than an exponential decay, we call the phenomenon as long-memory. In the literature, various studies have been conducted related to the long-memory process (Beran 1994; Granger and Ding 1996). Since the long-memory properties are commonly observed in stock returns, a large number of studies have been done in economics (Cheung and Lai 1995; Bollerslev and Mikkelsen 1996; Al-Yahyaee, Mensi, and Yoon 2018). On the other hand, the behaviour of stock market co-movement is a crucial issue in finance, and correlation/coherence analysis for these data has also been studied (Longin and Solnik 1995; Berben and Jansen 2005; Aloui and Hkiri 2014). However, only a few studies investigate coherency for long-memory processes as far as we know.

In this study, along the line of Li (2010), we investigate a robust coherence analysis for long-memory processes that can significantly extend the scope of robust coherence analysis, which is the main contribution of this study. Furthermore, we provide a theoretical background of Laplace cross-periodogram for long-memory processes.

The rest of this paper is organized as follows. In Section II, we briefly review the conventional coherence analysis and the Laplace cross-periodogram. Laplace cross-periodogram for long-memory

CONTACT Hee-Seok Oh heeseok.oh@gmail.com Department of Statistics,Seoul National University, Seoul 08826, Korea

processes and its theoretical property are discussed in Section III. Section IV presents numerical experiments, including real data analysis about money supply growth. Concluding remarks are given in Section V.

II. Coherence analysis

Ordinary coherence analysis

Suppose that we have jointly stationary and mean zero real-valued time series $\{Y_{jt}\}$, $\{Y_{kt}\}$, $t = 1, 2, \ldots, n$. The cross-spectrum of the two series is defined by the Fourier transform of the cross-covariance function $\gamma_{jk}(h) := E(Y_{j,t+h}Y_{k,t})$,

$$f_{jk}(\omega) := \frac{1}{2\pi}\sum_{h=-\infty}^{\infty}\gamma_{jk}(h)\exp(-i\omega h), \quad -\pi \le \omega \le \pi,$$

under the assumption that the cross-covariance function is absolutely summable. The cross-spectrum is a complex function as

$$\begin{aligned} f_{jk}(\omega) &= \frac{1}{2\pi}\sum_{h=-\infty}^{\infty}\gamma_{jk}(h)\exp(-i\omega h) \\ &= \frac{1}{2\pi}\sum_{h=-\infty}^{\infty}\gamma_{jk}(h)\cos(\omega h) \\ &\quad - i\frac{1}{2\pi}\sum_{h=-\infty}^{\infty}\gamma_{jk}(h)\sin(\omega h) \\ &= c_{jk}(\omega) - iq_{jk}(\omega), \end{aligned}$$

where $c_{jk}(\omega)$ and $q_{jk}(\omega)$ are called *cospectrum* and *quadrature spectrum*, respectively. The cospectrum measures the extent to which the series oscillate with the same phase, and the quadrature spectrum measures the extent to which they oscillate with a phase difference of a quarter cycle in either direction.

The coherence (or the squared coherency spectrum) at frequency ω of the series $\{Y_{jt}\}$ and $\{Y_{kt}\}$ is defined by

$$\mathcal{K}_{jk}^2(\omega) = \frac{|f_{jk}(\omega)|^2}{f_{jj}(\omega)f_{kk}(\omega)} \qquad j \neq k. \tag{1}$$

The coherence $\mathcal{K}_{jk}^2(\omega)$ denotes square of the correlation coefficient between ω-components of $\{Y_{jt}\}$ and $\{Y_{kt}\}$. By Cauchy–Schwarz inequality, it can be easily shown that $0 \le |\mathcal{K}_{jk}^2(\omega)| \le 1$, and a value of $\mathcal{K}_{jk}^2(\omega)$ close to 1 implies that the ω-components of the two series are strongly linearly related.

In general, for jointly stationary and mean zero real-valued time series $\{Y_{jt}, t = 1, \ldots, n\}$ $(j = 1, \ldots, p)$, the matrix of periodograms is defined as

$$\boldsymbol{I}(\omega) := [\mathcal{I}_{jk}(\omega)]_{j,k=1}^{p} = z(\omega)\, z^H(\omega),$$

where $z(\omega) := [Z_1(\omega), \ldots, Z_p(\omega)]^T$, $\mathcal{I}_{jk}(\omega) := Z_j(\omega)Z_k^H(\omega)$, and

$$Z_j(\omega) = \frac{1}{\sqrt{n}}\sum_{t=1}^{n} Y_{jt}\exp(-it\omega)$$

is the Fourier transform of $\{Y_{jt}\}$. Note that the superscript H denotes the complex conjugate transpose. The coherence of (1) can then be estimated by the following squared ratio of cross-periodogram and periodograms,

$$\frac{|\mathcal{I}_{jk}(\omega)|^2}{\mathcal{I}_{jj}(\omega)\mathcal{I}_{kk}(\omega)}.$$

In order to reduce the variability of periodograms, various smoothed periodograms have been used. The general form of a smoothed periodogram is

$$\hat{\mathcal{I}}(\omega_\ell) := \sum_{\ell'=-m}^{m} W_{\ell'}\mathcal{I}(\omega_{\ell-\ell'}), \tag{2}$$

where $\mathcal{I}(\omega)$ denotes a raw periodogram and W_ℓ denotes nonnegative weights that sum up to one. In this study, we employ the modified Daniell-kernel with the span of filter m (Bloomfield 2000). Hence, the coherence is estimated by

$$\hat{\mathcal{K}}_{jk}^2(\omega) = \frac{\hat{\mathcal{I}}_{jk}^2(\omega)}{\hat{\mathcal{I}}_{jj}(\omega)\hat{\mathcal{I}}_{kk}(\omega)}. \tag{3}$$

Robust coherence analysis

It is well known that ordinary coherence analysis performs well under a Gaussian assumption; hence, it is sensitive to outliers. To alleviate this problem, Li (2010) proposed Laplace cross-periodogram for robust coherence analysis. The Laplace cross-periodogram is defined as

$$\boldsymbol{L}(\omega) := [\mathcal{L}_{jk}(\omega)]_{j,k=1}^{p} = \boldsymbol{u}(\omega)\ \boldsymbol{u}^{H}(\omega), \tag{4}$$

where $\boldsymbol{u}(\omega) := [U_1(\omega), \ldots, U_p(\omega)]^T$, $\mathcal{L}_{jk}(\omega) := U_j(\omega)U_k^H(\omega)$, and $U_j(\omega)$ denotes the Laplace-Fourier transform of $\{Y_{jt}\}$ which is defined by

$$U_j(\omega) = \frac{1}{2}\sqrt{n}\{\beta_{j1}(\omega) - i\beta_{j2}(\omega)\}.$$

Here, β_j denotes a solution of the following least-absolute-deviations (LAD)

$$\beta_j(\omega) := [\beta_{j1}(\omega), \beta_{j2}(\omega)]^T = \arg\min_{\beta\in\mathbb{R}^2} \sum_{t=1}^{n} |Y_{jt} - \psi_t^T(\omega)\beta|, \tag{5}$$

where $\psi_t(\omega) := [\cos(\omega t), \sin(\omega t)]^T$. On replacing the LAD criteria in (5) by the least square, $\boldsymbol{L}(\omega)$ becomes identical to the ordinary cross-periodogram $\boldsymbol{I}(\omega)$.

For robust coherence analysis of two time series $\{Y_{jt}\}$ and $\{Y_{kt}\}$, we further consider a smoothed Laplace cross periodogram $\hat{\mathcal{L}}_{jk}(\omega_\ell)$ as in (2) and the corresponding estimator of the robust coherence $\boldsymbol{\Gamma}(\omega)$ can be defined as

$$\Gamma_{jk}^2(\omega) := \frac{\hat{\mathcal{L}}_{jk}^2(\omega)}{\hat{\mathcal{L}}_{jj}(\omega)\hat{\mathcal{L}}_{kk}(\omega)}. \tag{6}$$

III. Laplace coherence analysis of long-memory processes

For any fixed j, we consider a stationary process with mean zero and unit variance $\{Y_{jt}, t = 1, \ldots, n\}$. Then, the process $\{Y_{jt}\}$ is said to be long-memory, if there exists $d_j \in (0, 1/2)$ such that the spectral density at the origin can be represented as

$$f_j(\omega) \sim C_j \omega^{-2d_j} \text{as} \omega \to 0^+, \tag{7}$$

where $C_j > 0$ and d_j is called the *long-memory parameter*. It can be also defined by the correlation function as

$$\rho_j(h) := \mathrm{Corr}(Y_{j,t+h}, Y_{j,t}) \sim c_j(h) h^{2d_j - 1} \quad \text{as} \quad h \to \infty, \tag{8}$$

where $c_j(h)$ is positive for large h and varies slowly at infinity. A common example of long-memory processes is the fractionally integrated white noise and fractionally integrated ARMA (FARIMA) models. In these models, the parameter d_j corresponds to the integration order. A long-memory process can be defined as a short-memory process for $d_j = 0$, and generally, the process is stationary if $d_j < 1/2$ and invertible if $d_j > -1/2$. A stationary process with $d_j \in (0, 1/2)$ is characterized as a long-memory process.

We now derive the asymptotic distribution of the Laplace cross-periodogram for a long-memory process. We assume that the process is modelled as $Y_{jt} = \psi_t^T \beta_0 + \epsilon_{jt} (t = 1, \ldots, n)$, where $\epsilon_{jt} := G_j(Z_{jt})$, G_j is a measurable function from $\mathbb{R}$ to $\mathbb{R}$, and $\{Z_{jt}\}$ is a stationary mean zero and unit variance Gaussian process that satisfies the long-memory property of (7). We further consider the following assumptions for the asymptotic results of a Laplace cross-periodogram under multiple long-memory processes $\{Y_{jt}, t = 1, \ldots, n\}$ $(j = 1, \ldots, p)$.

- (C1) $(\boldsymbol{\Psi}^T\boldsymbol{\Psi})^{-1}$ exists for all $n \geq p$, where $\boldsymbol{\Psi}$ denotes an $n \times p$ matrix whose t-th row is ψ_t^T.
- (C2) $\max_t n^{1/2} \|\psi_t^T D^{-1}\| = O(1)$, where $D = (\boldsymbol{\Psi}^T\boldsymbol{\Psi})^{1/2}$.
- (C3) The cumulative distribution of $\{Y_{jt}\}$, F_{jt} has a uniformly continuous density function f_{jt} on $\Omega := \{x \in \mathbb{R} : 0 < F_{jt}(x) < 1\}$ such that $f_{jt} > 0$ almost everywhere on Ω, is positive and continuous at 0, and $F_{jt}(0) = 1/2$.
- (C4) For any given j and k, $\{Y_{jt}\}$ and $\{Y_{kt}\}$ are jointly stationary in the zero crossings in the sense that $P\{Y_{jt}Y_{ks} < 0\} = \varpi^{jk}(t - s)$ for all t and s.
- (C5) The function G is strictly monotonic and has a finite Fisher information.

Theorem 3.1. *Under the assumptions (C1)-(C5), the time series* $\{Y_{jt}, t = 1, \ldots, n\}$ $(j = 1, \ldots, p)$ *are observed from the model* $Y_{jt} = \psi_t^T \beta_0 + \epsilon_{jt}$, *where* $\epsilon_{jt} := G_j(Z_{jt})$, G_j *is a measurable function, and* $\{Z_{jt}\}$ *is a stationary mean zero and unit variance Gaussian process that satisfies the long-memory property of* (7). *Let* $\boldsymbol{\delta} := (\boldsymbol{\delta}_{inv}\boldsymbol{\delta}_{inv}^T)$, *where* $\boldsymbol{\delta}_{inv} = [\delta_{1,n}^{-1}, \ldots, \delta_{p,n}^{-1}]^T$,

$\delta_{j,n} := n^{(1-d_j)/2}|c_j^{1/2}(n)|$, d_j is a long-memory parameter, and $c_j(n)$ is a slowly varying function of $\{Z_{jt}\}$ defined in (8). From $\mathbf{L}(\omega) = \boldsymbol{u}(\omega)\boldsymbol{u}^H(\omega)$, we define $\tilde{\boldsymbol{u}}(\omega) := [\delta_{1,n}^{-1} U_1(\omega), \ldots, \delta_{p,n}^{-1} U_p(\omega)]^T$. Then, as $n \to \infty$,

$$\delta^{-1/2}\tilde{\boldsymbol{u}}(\omega) \sim N_c(\mathbf{0}, [\Upsilon_{jk}(\omega)]_{j,k=1}^p),$$

where $\Upsilon_{jk} := [\lambda_{jk}s_{jk}(\omega)]$ with $\lambda_{jk} = 1/(4f_j(0)f_k(0))$ and $s_{jk}(\omega) := \sum_{h=-\infty}^{\infty}\{1 - 2\varpi^{jk}(h)\}\exp(-ih\omega)$.

(9) *Proof.* From the results of Corollary 2 in Koul and Mukherjee (1993), we have

$$\delta_{j,n}^{-1}\boldsymbol{D}(\beta_j^{lad} - \beta_0) = \{f_j(0)\}^{-1}(\delta_{j,n}\boldsymbol{D})^{-1} \sum_t \psi_t\left\{\frac{1}{2} - I(\epsilon_{jt} \le 0)\right\} + o_p(1), \quad (9)$$

where β_j^{lad} denotes the coefficients of the LAD in (5). Since ψ_t is the harmonic regressor, we obtain $\boldsymbol{\Psi}^T\boldsymbol{\Psi} := \sum_{t=1}^n \psi_t(\omega)\psi_t^T(\omega) = (n/2)\mathbf{I} + o(1)$, which implies $\boldsymbol{D} \to \sqrt{n/2}\mathbf{I}$. In addition, since $\beta_0 = \mathbf{0}$, it follows that the result (9) becomes

$$\delta_{j,n}^{-1}\sqrt{2}U_j(\omega) = \delta_{j,n}^{-1}\sqrt{\frac{n}{2}}\{\beta_{j1}^{lad}(\omega) - i\beta_{j2}^{lad}(\omega)\} = \{f_j(0)\}^{-1}\delta_{j,n}^{-1}\sqrt{\frac{2}{n}}\sum_t \eta(\epsilon_{jt})e^{-it\omega} + o_p(1)$$

By letting $\boldsymbol{\xi}_j(\omega) := \frac{1}{\sqrt{n}}\sum_t \eta(\epsilon_{jt})e^{-it\omega}$, we further derive

$$\delta_{j,n}^{-1}\sqrt{2}U_j(\omega) = \delta_{j,n}^{-1}\sqrt{2}\{f_j(0)\}^{-1}\boldsymbol{\xi}_j(\omega) + o_p(1).$$

Then for $\boldsymbol{\xi}(\omega) := [\boldsymbol{\xi}_1(\omega), \ldots, \boldsymbol{\xi}_p(\omega)]^T$, it follows that

$$\lim_{n\to\infty} E\{\boldsymbol{\xi}(\omega)\boldsymbol{\xi}(\omega)^H\} = \frac{1}{4}[s_{jk}(\omega)]_{j,k=1}^p,$$

where $s_{jk}(\omega) := \sum_{h=-\infty}^{\infty}\{1 - 2\varpi^{jk}(h)\}\exp(-ih\omega)$. By the central limit theorem, we obtain $\boldsymbol{\xi}(\omega) \to N_c(\mathbf{0}, 1/4[s_{jk}(\omega)]_{j,k=1}^p)$, and for $\tilde{\boldsymbol{u}}(\omega) = [\delta_{1,n}^{-1} U_1(\omega), \ldots, \delta_{p,n}^{-1} U_p(\omega)]^T$,

$$\boldsymbol{\delta}^{-1/2}\tilde{\boldsymbol{u}}(\omega) \sim N_c(\mathbf{0}, [\Upsilon_{jk}(\omega)]_{j,k=1}^p).$$

IV. Numerical experiments

Simulation study

Example 1 We consider two long-memory processes that follow the models, namely

$$X_t = 2a_t + \epsilon_{1t}$$

$$Y_t = a_t\epsilon_{2t},$$

where $\{a_t\}$ is a nonnegative periodic sequence of the form $1.0 + 0.9\cos(\omega_0 t)$ with $\omega_0 = 2\pi \times 0.1$, and ϵ_{1t} and ϵ_{2t} are independent FARIMA(0, 0.3, 0) processes with three different error distributions: Gaussian distribution, t-distribution with 2.1 degrees of freedom, and Cauchy distribution with a scale parameter of 0.25. For each combination of $\{X_t\}$ and $\{Y_t\}$, the noise type, and $n = 600, 1000$ datasets are generated. For each generated dataset, the ordinary and Laplace coherence are performed. Note that the ordinary coherence is computed by (3) and the Laplace coherence is computed by (6). Figure 1 shows the averages of ordinary and Laplace coherences according to the noise type. Overall, the Laplace coherence efficiently detects the common frequency of ω_0. Especially, for the heavy-tailed noise distributions, the Laplace coherence outperforms the ordinary coherence in terms of identifying the frequency information ω_0 while retaining its robustness.

Example 2 Let $\{X_t\}$ be a FARIMA(2, 0.3, 0) process with parameters $\boldsymbol{\phi}_1 = 1.2\cos(2\pi \times 0.25)$ and $\boldsymbol{\phi}_2 = -(0.6)^2$ (McLeod, Yu, and Krougly 2007). We consider the following two time series

$$Y_{1t} = c_1(X_t + \epsilon_{t1})$$

$$Y_{2t} = c_2(\alpha X_{t-5} + \epsilon_{t2}),$$

where ϵ_{t1} and ϵ_{t2} are mutually independent i.i.d. white noise $N(0, 3.162)$, and the scale parameters c_1 and c_2 are chosen such that $\mathrm{Var}(X_t) = \mathrm{Var}(Y_t) = 1$. By following the approach of Li (2010), we try to detect the common component in the two series $\{Y_{1t}\}$ and $\{Y_{2t}\}$ by coherence analysis. For this purpose, we perform the following hypothesis testing $H_0 : \alpha = 0$ vs. $H_1 : \alpha \neq 0$ with the rejection rule: reject H_0 if the maximum absolute coherency is higher than a threshold.

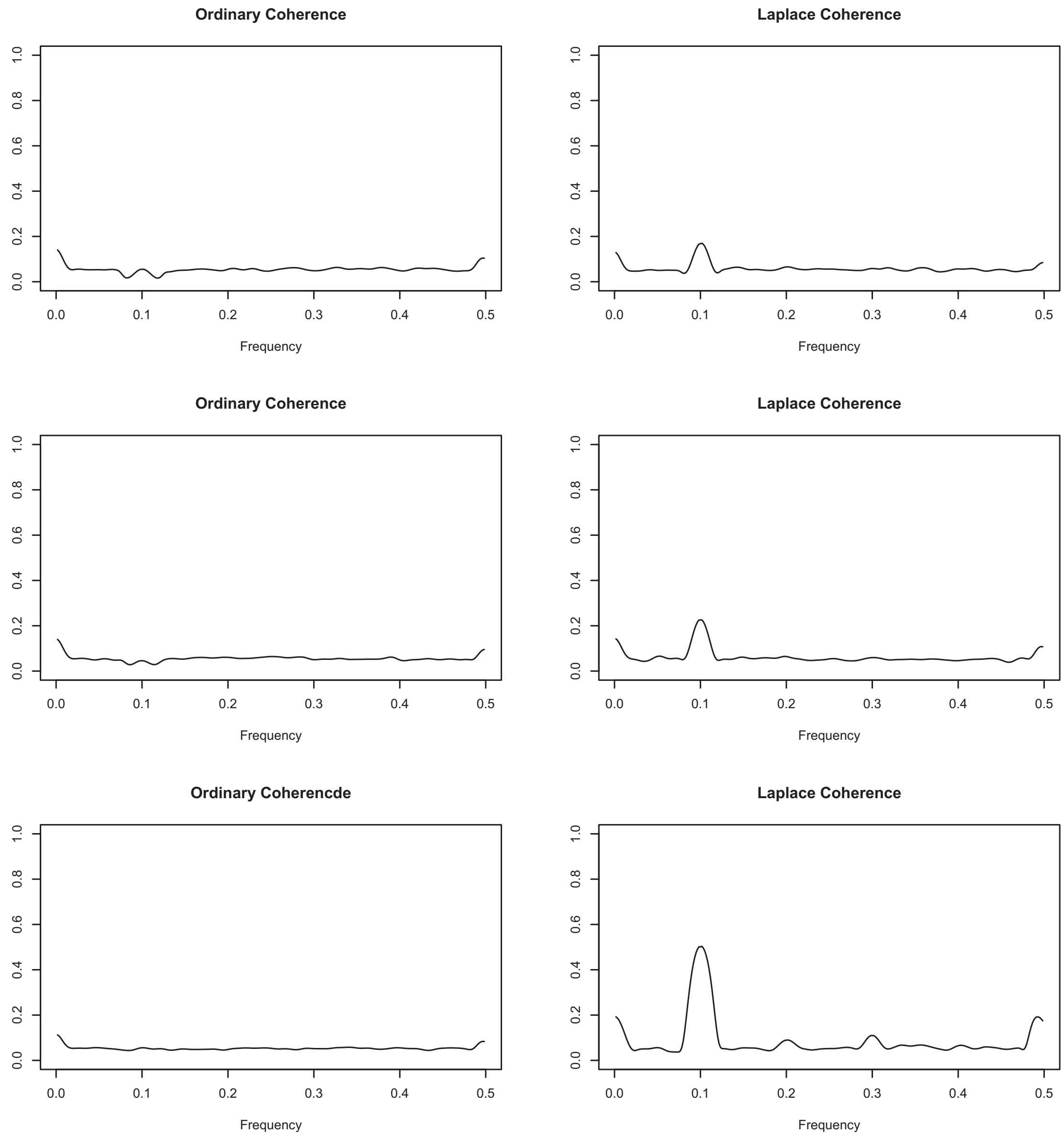

Figure 1. Averages of ordinary coherences and Laplace coherences in Example 1: (top) Gaussian distributed error model, (middle) *t* distributed error model, and (bottom) Cauchy distributed error model.

For evaluation, we consider the receiver operating characteristic (ROC) curve of a binary classifier system. The ROC curve depicts the relative trade-off between benefits and costs. Therefore, a point in a ROC curve is more suitable than another if it is located in the upper-left area.

We generate 1000 data sets. Among them, the first 500 data sets are generated with $\alpha = 0$, and the next 500 data sets are generated with $\alpha \neq 0$. Further, we consider four noise types: (G) Gaussian, (LG) log gamma with shape parameter 1 and scale parameter 2 (Hogg and Klugman 2009), and (C) Cauchy distribution with scale parameter 0.25. Figure 2 shows the ROC curves for the ordinary and Laplace coherence analyses under the four noise scenarios. It can be seen that the Laplace coherence outperforms the ordinary one for non-Gaussian distributed noise cases.

Real data example: money supply growth

We analyse the monthly measures of the monetary aggregates from January 1959 to May 2018 obtained from https://www.federalreserve.gov/releases/h6/about.htm. M1 consists of easily accessible money,

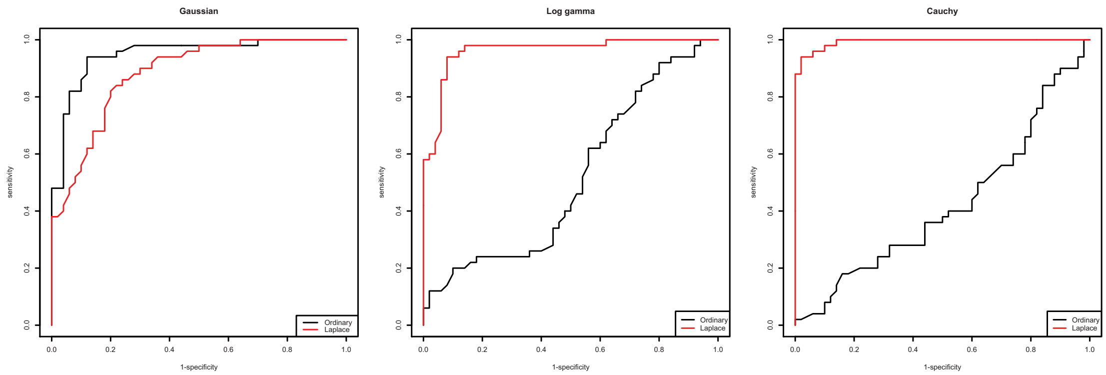

Figure 2. ROC curves of the maximum absolute coherency test by the ordinary coherency (black) and the Laplace coherency (red) under different noise distributions: Gaussian, log gamma, and Cauchy distribution. The results are based on 1,000 simulated data sets.

such as currency and demand deposits, whereas M2 consists of money that requires more time for access, such as savings deposits and money market accounts. Since M1 is included in M2, we consider the non-M1 components of M2, which are primarily household holdings of savings deposits, small time deposits, and retail money market mutual funds (Sela and Hurvich 2012). The non-M1 components of M2 are denoted as M1(M2). Figure 3 shows the log differences of two time-series. Further, from the periodograms in Sela and Hurvich (2012), it is seen that the two series are long-memory processes. Figure 4 shows the ordinary and Laplace coherency plots. For the result of the ordinary coherence, the main peak occurs around a frequency of 0.05, which corresponds to a period of nearly 20 months, and some minor peaks appear over other frequencies. On the other hand, Laplace coherence provides two main peaks; one is around 0.05, and the other appears near the frequency of 0.35, which corresponds to a period of just under 3 months.

For the evaluation of this peak, we obtain the Laplace periodograms of Li (2008) for the two time series M1 and M1(M2), which are displayed in Figure 5. We note that the Laplace periodogram is a robust version of the ordinary periodogram and can be obtained from the Laplace coherence with $j = k = 1$ in (4). It can be seen that there is a common peak near 0.35 as well. We finally remark that this frequency can also be identified by the ordinary coherence, but it is not distinct, compared to other frequencies, whereas the peak can be easily detected by the Laplace coherence.

V. Concluding remarks

In this paper, we have considered a robust coherence analysis for long-memory processes based on Laplace cross-periodogram. We have investigated the asymptotic distribution of

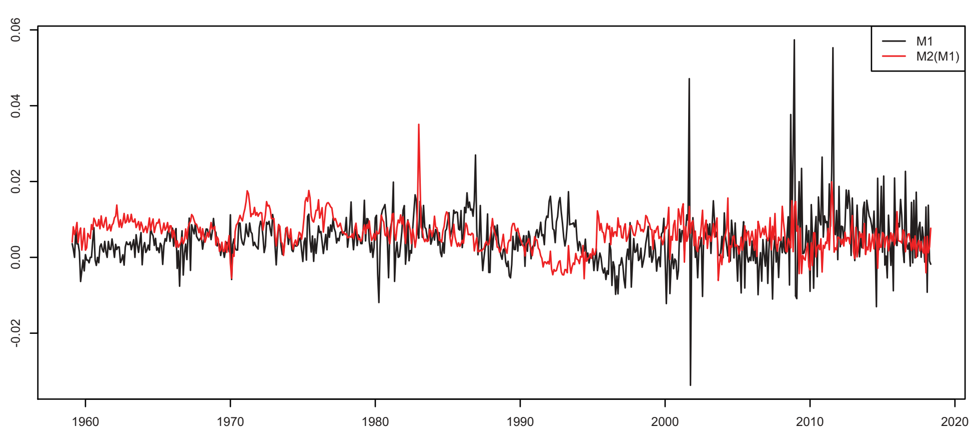

Figure 3. Log differences of M1 and M2(M1).

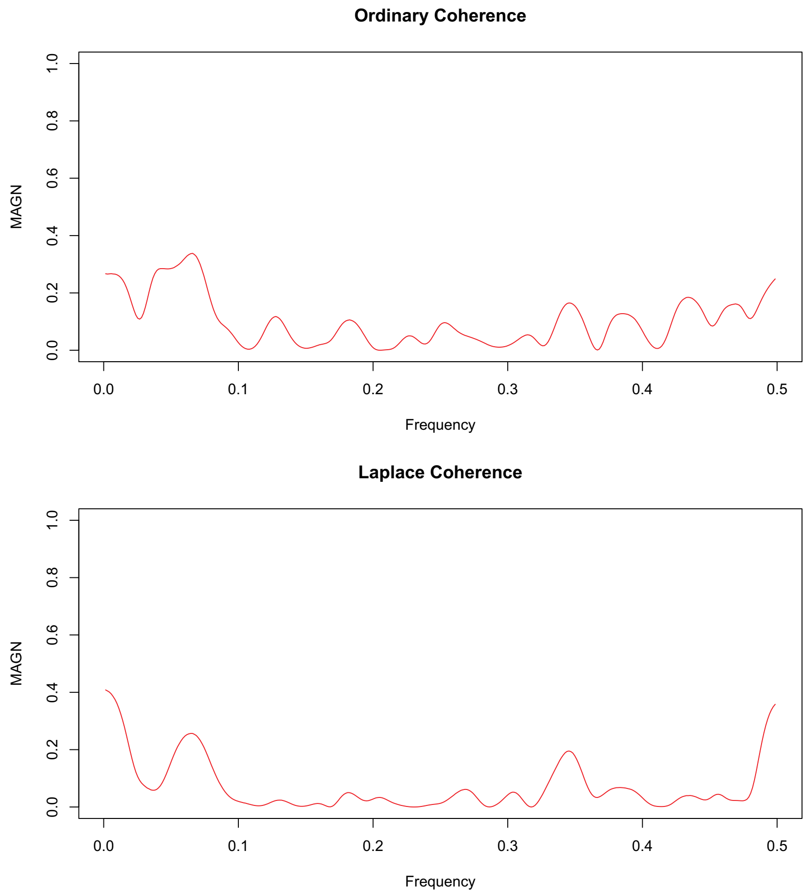

Figure 4. Ordinary coherency and Laplace coherency of M1 and M2(M1).

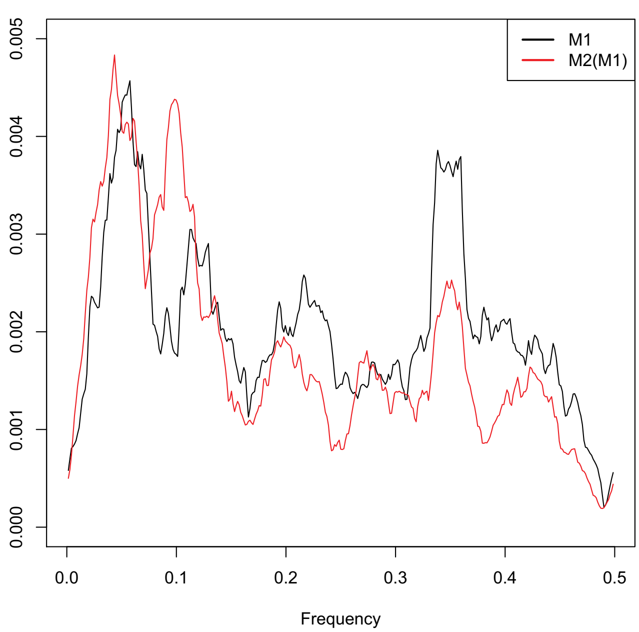

Figure 5. Laplace periodograms of M1 and M2(M1).

Laplace cross-periodogram to justify the utility of Laplace cross-periodogram-based coherence analysis. We believe that this is the main contribution of this paper. In addition, we have conducted simulated examples, showing that the proposed robust coherence analysis is capable of understanding the linear relationships between two long-memory processes in the frequency domain. Furthermore, we have performed real data analysis for money supply growth and successfully detected two main peaks between two long-memory monetary-related processes. For possible future research, the Laplace cross-periodogram is worth extending to a quantile cross-periodogram for long-memory processes. Quantile cross-periodogram may reveal hidden relationships between two long-memory processes, which can provide a richer interpretation of the time-series data compared to the Laplace cross-periodogram.

Disclosure statement

No potential conflict of interest was reported by the authors.

Funding

This research was supported by the National Research Foundation of Korea (NRF) grant funded by the Korea government [NRF-2019R1A2C4069453 and NRF-2018R1D1A1B07042933].

ORCID

Yaeji Lim http://orcid.org/0000-0002-8698-8667

References

Aloui, C., and B. Hkiri. 2014. "Co-movements of GCC Emerging Stock Markets: New Evidence from Wavelet Coherence Analysis." *Economic Modelling* 36: 421–431. doi:10.1016/j.econmod.2013.09.043.

Al-Yahyaee, K. H., W. Mensi, and S. M. Yoon. 2018. "Efficiency, Multifractality, and the Long-memory Property of the Bitcoin Market: A Comparative Analysis with Stock, Currency, and Gold Markets." *Finance Research Letters* 27: 228–234. doi:10.1016/j.frl.2018.03.017.

Beran, J. 1994. *Statistics for Long-Memory Processes*. Boca Raton: Chapman and Hall/CRC.

Berben, R. P., and W. J. Jansen. 2005. "Comovement in International Equity Markets: A Sectoral View." *Journal of International Money and Finance* 24 (5): 832–857. doi:10.1016/j.jimonfin.2005.04.001.

Bloomfield, P. 2000. *Fourier Analysis of Time Series: An Introduction*. 2nd ed. New York: John Wiley & Sons.

Bollerslev, T., and H. O. Mikkelsen. 1996. "Modeling and Pricing Long Memory in Stock Market Volatility." *Journal of Econometrics* 73 (1): 151–184. doi:10.1016/0304-4076(95)01736-4.

Carter, G. C. 1987. "Coherence and Time Delay Estimation." *Proceedings of the IEEE* 75: 236–255.

Cheung, Y. W., and K. S. Lai. 1995. "A Search for Long Memory in International Stock Market Returns." *Journal of International Money and Finance* 14 (4): 597–615. doi:10.1016/0261-5606(95)93616-U.

Govindan, R. B., J. Raethjen, F. Kopper, J. C. Claussen, and G. Deuschl. 2005. "Estimation of Time Delay by Coherence Analysis." *Physica A: Statistical Mechanics and Its Applications* 350 (2–4): 277–295. doi:10.1016/j.physa.2004.11.043.

Granger, C. W., and Z. Ding. 1996. "Varieties of Long Memory Models." *Journal of Econometrics* 73 (1): 61–77. doi:10.1016/0304-4076(95)01733-X.

Grinsted, A., J. C. Moore, and S. Jevrejeva. 2004. "Application of the Cross Wavelet Transform and Wavelet Coherence to Geophysical Time Series." *Nonlinear Processes in Geophysics* 11: 561–566. doi:10.5194/npg-11-561-2004.

Hogg, R. V., and S. A. Klugman. 2009. *Loss Distributions*. New York: John Wiley & Sons.

Koul, H. L., and M. Mukherjee. 1993. "Asymptotics of R-, MD- and LAD-estimators in Linear Regression Models with Long Range Dependent Errors." *Probability Theory and Related Fields* 95: 535–553. doi:10.1007/BF01196733.

Li, T.-H. 2008. "Laplace Periodogram for Time Series Analysis." *Journal of the American Statistical Association* 103: 757–768. doi:10.1198/016214508000000265.

Li, T.-H. 2010. "Robust Coherence Analysis in the Frequency Domain." *Proceedings of the European Signal Processing Conference (EUSIPCO)*. 368–371.

Longin, F., and B. Solnik. 1995. "Is the Correlation in International Equity Returns Constant: 1960–1990?" *Journal of International Money and Finance* 14 (1): 3–26. doi:10.1016/0261-5606(94)00001-H.

Maharaj, E. A., and P. D'Urso. 2010. "A Coherence-based Approach for the Pattern Recognition of Time Series." *Physica A: Statistical Mechanics and Its Applications* 389 (17): 3516–3537. doi:10.1016/j.physa.2010.03.051.

McLeod, A. I., H. Yu, and Z. L. Krougly. 2007. "Algorithms for Linear Time Series Analysis: With R Package." *Journal of Statistical Software* 23: 1–26. doi:10.18637/jss.v023.i05.

Sela, R. J., and C. M. Hurvich. 2012. "The Averaged Periodogram Estimator for a Power Law in Coherency." *Journal of Time Series Analysis* 33: 340–363. doi:10.1111/jtsa.2012.33.issue-2.

Sun, F. T., L. M. Miller, and M. D'Esposito. 2004. "Measuring Interregional Functional Connectivity Using Coherence and Partial Coherence Analyses of fMRI Data." *Neuroimage* 21: 647–658. doi:10.1016/j.neuroimage.2003.09.056.